Chemical Engineering Journal 317 (2017) 394–403

Contents lists available at ScienceDirect

Chemical Engineering Journal

journal homepage: www.elsevier.com/locate/cej

Catalytic paper made from ceramic fibres and natural ulexite. Application to diesel particulate removal

Sabrina A. Leonardi [a,b], Miguel A. Zanuttini [b], Eduardo E. Miró [a], Viviana G. Milt [a,*]

[a] Instituto de Investigaciones en Catálisis y Petroquímica, INCAPE (FIQ, UNL – CONICET), Santiago del Estero 2829, S3000AOJ, Santa Fe, Argentina
[b] Instituto de Tecnología Celulósica (ITC), FIQ, UNL, Santiago del Estero 2654, S3000AOJ, Santa Fe, Argentina

HIGHLIGHTS

- Purification of natural ulexite extracted from an Argentinean deposit.
- Papermaking process to obtain mechanically-resistant ceramic paper using ulexite as binder of ceramic fibres.
- Replacement of colloidal suspensions by ulexite as binder of ceramic fibres.
- Addition of Co to promote soot oxidation through its redox capacity.
- Incorporation of Ba or La to trap NOx and to yield reactive oxygen to the Co-soot centres.

GRAPHICAL ABSTRACT

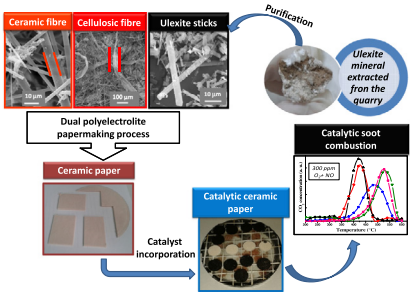

ARTICLE INFO

Article history:
Received 26 October 2016
Received in revised form 1 February 2017
Accepted 4 February 2017
Available online 6 February 2017

Keywords:
Natural ulexite
Binder properties
Ceramic paper
Fibrous-structured catalysts
Soot removal

ABSTRACT

Ceramic paper discs were made by employing a dual papermaking technique and by partially substituting cellulosic fibres by SiO_2-Al_2O_3 ceramic ones. Ulexite ($NaCaB_5O_6(OH)_6{\cdot}5(H_2O)$), extracted from the natural mineral, was added as a binder to give ceramic paper the necessary strength for its manipulation and catalytic use.

Either La,Co or Ba,Co was incorporated in order to give ceramic paper the capability of trapping NOx and oxidizing soot particles. Structured catalysts were characterised by SEM, FTIR and XRD, and the mechanical properties were also determined. Lanthanum was deposited on ceramic fibres as $La_2O_2CO_3$ aggregates and barium as $BaCO_3$ filaments, being cobalt deposited as Co_3O_4 flakes. Mechanical properties indicated that the ceramic paper obtained from natural ulexite proved to be stronger, though less flexible than those prepared using colloidal suspensions as a binder.

Diesel soot oxidation activity was determined by TPO either adding or not 0.1% NO into the feeding stream. The thus prepared systems resulted in being active towards soot oxidation, being the value of maximum combustion rate 420 °C, which is within the temperature range of diesel exhaust gases.

1. Introduction

A great number of technologies applied to environmental remediation are based on catalytic processes in which activity and selectivity are key factors to enhance efficiency. These factors can be improved either by changing catalytic formulations or by varying the dispersion of active species, i.e. by modifying their physicochemical characteristics, and also by means of a suitable design of the reactor. With the aim of process intensification, new concepts for catalyst support structures appear to be attractive, apart from the long-established ones such as foams, monolith and pellets.

* Corresponding author.
E-mail address: vmilt@fiq.unl.edu.ar (V.G. Milt).

http://dx.doi.org/10.1016/j.cej.2017.02.013
1385-8947/

Many of these new structures involve the use of fibres which provide benefits to catalytic applications due to: (i) their high surface-to-volume ratio that allows a good deposition of catalytic components and (ii) the high void fractions offering a low flow pressure drop [1]. In addition, and depending on the preparation method, fibrous substrates can be arranged as versatile structures that can be easily fabricated and accommodated in various geometries. As a recent example, Liu et al. reported the synthesis of a hierarchical porous mullite fibre network for gas filtration [2].

Besides, ceramic paper constitutes a class of fibre arrangement in which the network of ceramic fibres interconnected through pore-type spaces benefits gas diffusion [3]. The employment of ceramic and cellulosic fibres during the papermaking process produces ceramic paper resistant to severe thermal conditions after calcination (temperatures above 900–1000 °C) [4]. To increase the retention of inorganic compounds during the wet mat formation of ceramic paper, a dual method that combines anionic and cationic polyelectrolytes can be used. The incorporation of proper binders during paper manufacturing is necessary to obtain fibrous structures easy to handle [5]. In this sense, an important challenging feature is their mechanical strength. Most reported works consider the use of colloidal suspensions (mainly Al_2O_3, CeO_2, or ZrO_2) as ceramic fibre binders [6–11]. As an alternative, we have recently reported the use of borate-type compounds [12].

Borate minerals are the main source of boron and have a multitude of industrial applications. Within a range of over 160 species of borate minerals, ulexite is one of the most important in commercial terms [13]. Ca,Na-borate minerals are mainly used for fibreglass making and also for the production of ceramics and ceramic glazes [14,15]. Besides, ulexite frit has been used to produce engobes for manufacturing ceramic tiles [16]. In a recent publication, Ozturk et al. [17] studied the addition of ulexite instead of boric acid to frit composition to modify thermal behaviour and surface properties of transparent wall tile glaze. Also, Guzel et al. have studied the use of colemanite and ulexite as novel fillers in epoxy composites [18].

During thermal treatments, ulexite goes through dehydration processes and suffers the loss of its crystallization water while undergoing various mineralogical and structural changes [19]. At temperatures higher than 600 °C, ulexite particles first agglomerate weakly keeping their shape and individuality, then this union gets stronger and takes on the appearance of a sinter. The fusion process occurs at a temperature higher than 800 °C and a homogeneous and fluid liquid is obtained after treatments at temperatures higher than 1000 °C [20].

As substitutes for colloidal binders, we studied the use of borates to join ceramic fibre in the matrix of ceramic paper. In comparison with colloidal suspensions, borates have the advantage of being cheaper and more easily obtained [21]. We tested nobleite ($CaB_6O_{10}{\cdot}4H_2O$), colemanite ($Ca_2B_6O_{11}{\cdot}5H_2O$) and anhydrous ulexite ($NaCaB_5O_9$) and although none of the borates used melted under calcination conditions, individual particles began to sinter as the calcination temperature increased, reinforcing the ceramic fibre network and thus, providing the ceramic paper with the necessary mechanical strength properties. It was found that after calcination at 650 °C, anhydrous ulexite supplied better strength and elasticity. In a subsequent contribution [5], we used anhydrous ulexite to prepare catalytic ceramic paper containing Pt-NaY zeolite used as CO oxidation catalysts. Light-off curves indicated that when incorporating the zeolitic component by spraying, the CO oxidation reaction occurred at ca. 130 °C, and the total CO conversion was achieved at 150 °C. However, commercial anhydrous ulexite crystals (BORAX), treated at 900 °C, had the vitreous structure of the frit material and a variable particle size, ranging from very small particles to ones of 125 μm. It was too difficult to decrease the particle size by milling. The variety of borate particle sizes ranging from ca. 1 to 100 μm made ceramic paper difficult to handle after calcination.

In a recent publication, S. Kutuk [22] studied the effect of milling parameters on the particle size of ulexite. The mechanical milling technique was performed by a high-energy ball-milling that allowed them to obtain nano-sized ulexite particles. This process involves two high-energy demanding steps: the first one lets them obtain anhydrous ulexite and the second one is needed for milling it. On the other hand, considering the fibrous nature of natural ulexite, in which fibre diameters are close to 1 μm, it is possible to use this material as a binder for ceramic fibres without the demanding high-energy milling process described above. In addition, the morphology of natural ulexite that fits into that of ceramic fibre may be more compatible with the papermaking process.

In this context, the aim of this work is to test natural ulexite ($NaCaB_5O_6(OH)_6{\cdot}5(H_2O)$) as a ceramic binder to enhance the mechanical properties of ceramic paper. Catalytic components were added to ceramic paper in order to give it the capacity of burning diesel soot particles, which constitutes one of the main contaminants emitted from Diesel engines [4,23]. The addition of basic elements, such as Ba or La, has been considered since they favour NOx adsorption and contribute to soot removal. Apart from mechanical properties, physicochemical ones were evaluated by XRD, XRF, FTIR, TGA and SEM whereas catalytic behaviour was studied by TPO experiments in order to evaluate the feasibility of the passive regeneration of systems.

2. Experimental

2.1. Binder conditioning

Ulexite was separated from the mineral extracted from an ore quarry in Salta, Argentina (BORAX S.A., Fig. 1S, Supplementary Information) firstly by sieving through an 80 mesh sieve in order to eliminate big SiO_2 grains. Then, the fine powder was milled and SiO_2 was removed by elutriation. To this aim, the sample was placed into a glass vessel filled with distilled water and it was submitted to an ultrasonic bath for 15 min. After 2 min of decanting, the supernatant was poured into a beaker to separate the settled material. This process was repeated twice. Finally, ulexite was dewatered and later dried in an oven at 130 °C during 24 h. The yield of the process was 30 wt% of natural ulexite. The "natural ulexite" thus obtained was the material used as a binder for ceramic fibres during the papermaking process.

On the other hand, a fraction of further pure ulexite was obtained using only the white portion of the mineral that constituted less than 5 wt% of the raw material (Fig. 1, "untreated pure ulexite"). The latter was submitted to the same procedure as described above. This material was denoted as "pure ulexite" and was considered to be a reference material.

2.2. Ceramic paper preparation

The papermaking technique developed by Ichiura et al. [24], which considers a dual polyelectrolyte retention system, was used for the preparation of ceramic paper. The procedure implies the use of cationic and anionic polymers. Two kinds of fibres were employed, cellulosic and ceramic ones, which after calcination led to the formation of ceramic paper discs suitable for high-temperature applications. In order to produce easy-to-handle paper, a pentaborate compound (ulexite, $NaCaB_5O_6(OH)_6{\cdot}5(H_2O)$), as previously described in Section 2.1, was added as a binder during ceramic paper manufacturing. Refractory ceramic fibres (RCF, 50 wt% SiO_2, 48 wt% Al_2O_3 and 2 wt% impurities) were obtained from a ceramic insulation mat from CARBO. The fibrous mat was

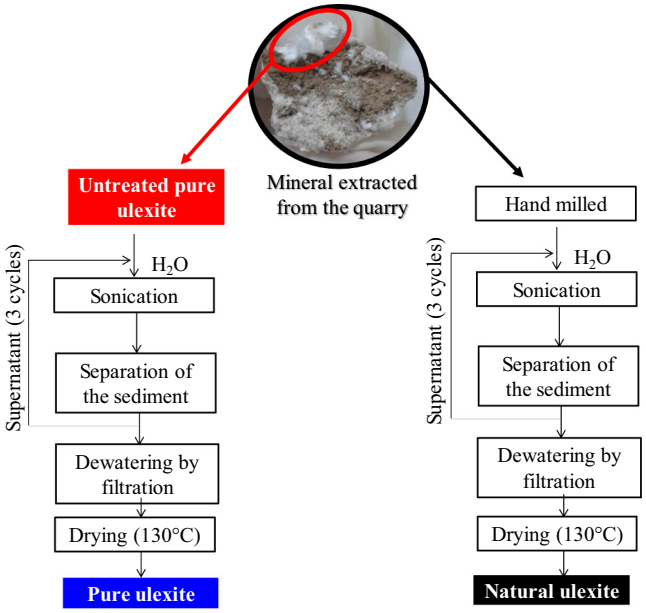

Fig. 1. Initial ulexite material extracted from the ore quarry. Scheme of fractions used and the way they were conditioned.

dispersed in tap water, and fibres were separated from low slenderness particles by an elutriation process. The yield of fibres was around 50%, with an average fibre length of 660 μm and an average diameter of 6 μm. Cellulosic fibres from a dried commercial bleached softwood Kraft pulp, were re-wetted for at least 24 h and dispersed by a standard disintegrator before use. Their characteristics (3 mm in length and ribbon shape with an average width of 30 μm) enhanced mat formation during the preparation procedure.

The cationic polymer was polyvinyl amine (PVAm) (Luredur PR 8095) from BASF, with a molecular weight of $4 \cdot 10^5$ g mol^{-1} and a charge density of 4.5 meq g^{-1}, and the anionic polymer was anionic polyacrylamide (A-PAM) from ASHLAND, with a molecular weight >2.10^6 g mol^{-1} and a charge density of 1.9 meq g^{-1}. Under

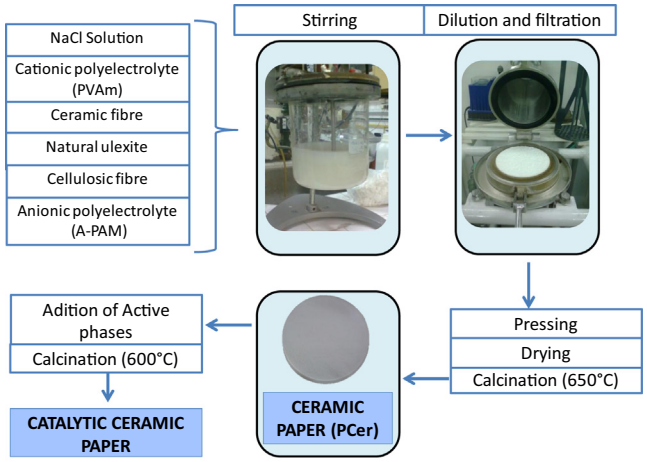

Fig. 2. Scheme of catalytic ceramic paper preparation.

gentle agitation of 1000 ml NaCl solution (0.01 N), 10 g of ceramic fibre was added. After 5 min of continuous stirring, 66 ml of PVAm solution (1 g.l^{-1}) was incorporated, then 4.0 g of ulexite and 1.50 g of cellulose fibre. Finally, 23 ml of A-PAM polymer solution (1.0 g. l^{-1}) was added. From this suspension, a handsheet was formed by the SCAN standard method (SCAN-C 26:76 and SCAN-M 5:76) but using tap water (180 mS) and applying the double of the standard pressing pressure (37.5 kPa). The pressing was carried out twice in order to remove as much water as possible. The wet sheet was dried under controlled conditions (23 °C and 50%RH) for 24 h and finally calcined in air for 2 h at 650 °C. Fig. 2 shows the scheme of ceramic paper preparation. The final ceramic paper obtained consisted of circular sheets, 160 mm in diameter and 2.5 mm thick and they were denoted as PCer.

2.3. Catalytic component addition

In order to develop structured catalysts, single or mixed solutions were used to incorporate La; La,Co; Ba or Ba,Co into ceramic

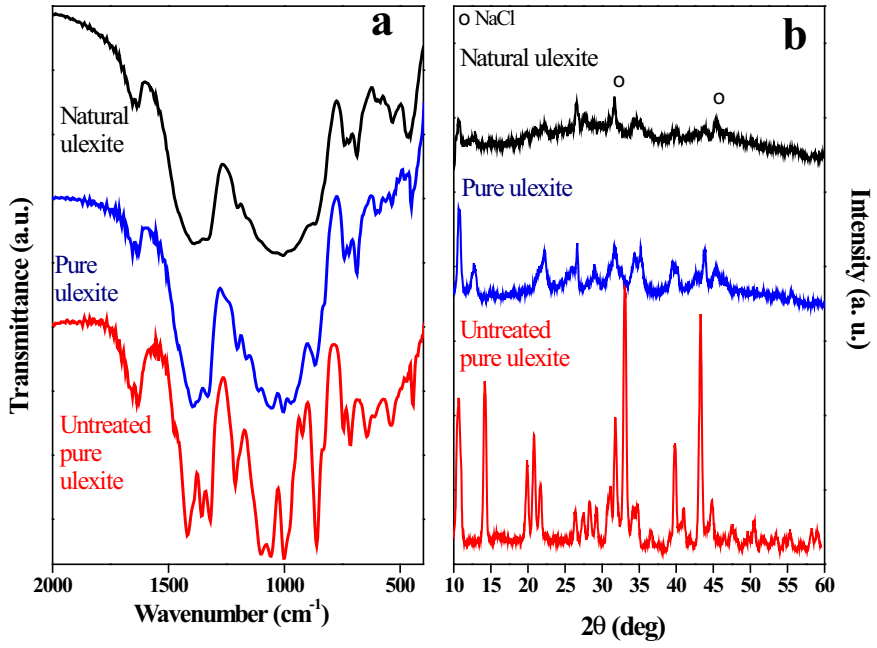

Fig. 3. (a) FTIR spectra and (b) XRD patterns of ulexite.

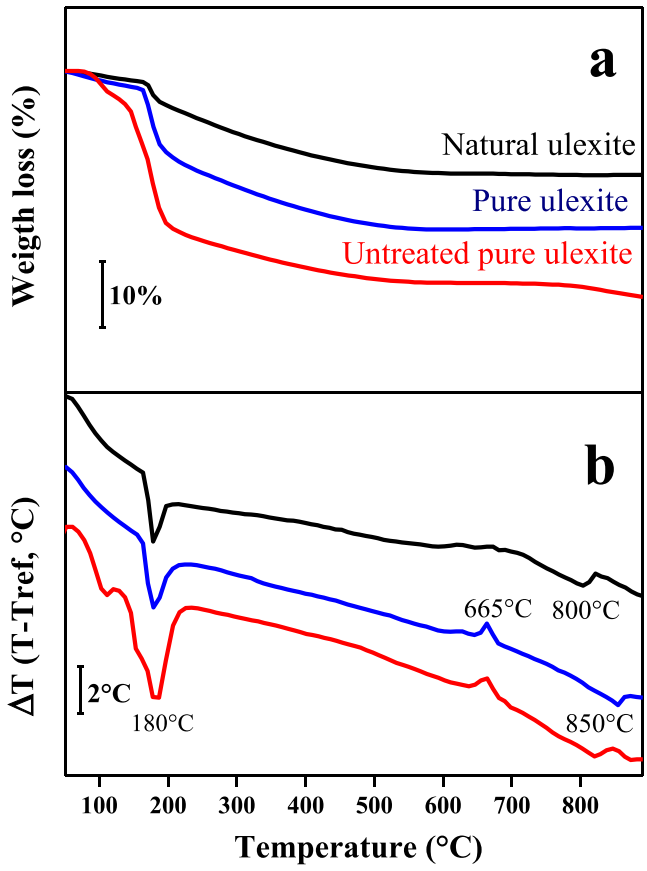

Fig. 4. (a) Thermal analysis, TGA and (b) SDTA experiments of natural ulexite. (Atmosphere: air and heating rate: 10 °C/min.)

paper. $La(NO_3)_3$ (38.12 g.l^{-1}) and $Ba(NO_3)_2$ (31.07 g.l^{-1}) were the single solutions used, whereas $La(NO_3)_3$ (38.12 g.l^{-1}) + $Co(NO_3)_2$ (50.75 g.l^{-1}) and $Ba(NO_3)_2$ (31.07 g.l^{-1}) + $Co(NO_3)_2$ (50.75 g.l^{-1}) were the corresponding mixed solutions employed. Ceramic paper discs/pieces were soaked up to saturation with the above mentioned solutions to load 12 wt% of each catalytic component after calcination at 600 °C for 2 h. The systems thus obtained were designated as PCer-La; PCer-La,Co; PCer-Ba and PCer-Ba,Co; respectively.

2.4. Characterisation

2.4.1. X-ray diffraction (XRD)

Crystalline phases were determined by means of a Shimadzu XD-D1 instrument with monochromator using CuKα radiation at a scan rate of 2°.min^{-1}, from 2θ = 10° to 80°. Ceramic paper pieces of about 2 cm × 2 cm were cut and supported in the special sample holder. The software package of the equipment was used for phase identification from X-ray diffractograms.

2.4.2. Infrared spectroscopy (FTIR)

Fourier Transform Infrared Spectroscopy (FTIR) was used to identify the functional groups. Samples were prepared in the form of pressed wafers (ca. 1% sample in KBr). A Shimadzu IR Prestige-21 spectrometer was utilized to obtain the infrared spectra. All spectra involved the accumulation of 40 scans at 8 cm^{-1} resolution.

2.4.3. X-ray fluorescence (XRF)

X-ray Fluorescence Spectrometry was carried out to determine the presence and to approximately quantify elements between Na23 and U92, using a Shimadzu Spectrometer (EDX-720). The quantification method used did not require standards.

2.4.4. Thermal analysis (TGA and SDTA)

Thermogravimetric analyses were performed to detect phase transformations of the catalysts during heating treatments in air using a Mettler Toledo TGA/SDTA 851 equipment. Usually, 10 mg of catalysts (non-calcined catalytic ceramic paper) was heated from 25 to 900 °C at 10 °C.min^{-1} in an air flow (20 ml.min^{-1}).

2.4.5. Scanning electron microscopy (SEM)

The morphology of ceramic paper was studied by Scanning Electron Microscopy (SEM) using an electronic microscope JEOL JSM-35C with an acceleration voltage of 20 kV. Samples were coated by sputtering them with a thin layer of Au in order to improve image quality.

2.4.6. Mechanical properties

The tensile strength and elastic modulus of ceramic paper were determined with an INSTRON 3344 universal tester, equipped with a load cell of 1000 N at a rate of 50.8 mm.min^{-1}, using the standard TAPPI T 576 pm-07 method, which is used for tissue paper. Ceramic paper sheets of about 2 mm thick were cut into 50 mm wide and 70 mm long rectangles, leaving a 50 mm free length between testing grips.

2.5. Catalytic evaluation

Soot particles were produced by burning a commercial diesel fuel (YPF, Argentina) in a glass vessel. After being collected from the vessel walls, the soot was dried in a stove at 120 °C for 24 h. In order to produce homogeneous suspensions, the soot particles were dispersed in n-hexane using an ultrasonic bath. Two different suspensions of soot in n-hexane were prepared (300 ppm and 600 ppm) to vary the amount of soot loaded. In this sense, soot was incorporated into ceramic paper discs of 1.6 cm in diameter and the suspension was added dropwise until complete impregnation, and then dried at room temperature for 24 h. The activity of catalytic ceramic paper for the combustion of soot was studied by temperature-programmed oxidation (TPO). For this purpose, the structured samples + soot (3 stacked discs) were heated at 5 °C.min^{-1} from room temperature up to 600 °C in O_2 (18%) + NO (0.1%) diluted in He (total flow 20 ml.min^{-1}) by means of a flow equipment designed for this purpose. Identical experiments, but without NO in the feed, were also carried out. The exhaust gases

Table 1
Weight loss [%] at different stages of thermogravimetric analysis, (calculated from Fig. 4).

Step	ΔT [°C]	Δw [%]		
		Theoretical	Pure ulexite	Natural ulexite
1	25–165	8.8	3.1	1.8
2	165–185	13.1	8.8	2.7
3	185–550	13.1	12.7	11.5
4	550–900	0	0	0

were analyzed with a Shimadzu GC-2014 chromatograph (with TCD detector). TPO results are reported as CO_2 normalized TCD peak area (CO_2 peak area measured at each temperature divided by the total area obtained during the TPO experiment).

3. Results and discussion

3.1. Ceramic fibre binder (ulexite) characterisation

Natural ulexite was characterised both chemically and morphologically in order to determine its composition and structure. Fig. 3a shows the FTIR spectra of the natural ulexite as well as the one used as reference. The latter (pure ulexite) exhibited all the IR signals expected for ulexite ($NaCa[B_5O_6(OH)_6]\cdot 5(H_2O)$) [25]. In addition, the signals at 612 and 2367 cm^{-1} can be assigned to $LiB_5O_8\cdot 5H_2O$ This is not surprising if K, Li, Mg and Al are considered to be present in the ulexite ore quarry. XRF analysis revealed that natural ulexite contained Al_2O_3 (7.5%), Fe_2O_3 (4.0%), MgO (4.0%), Cl (2.0%), and K_2O (1.6%) in addition to Na_2O (18.5%) and CaO (61.5%). Besides, small quantities (<0.3%) of TiO_2 and SO_3 were detected, though the technique could not detect Li.

In most outcrops other minerals, mainly halite (NaCl) and gypsum ($CaSO_4\cdot 2H_2O$) also occur [13]. In addition, if polyborate anions are regarded as consisting of various BO_3 planar triangles and BO_4 tetrahedrons [25], borates containing different numbers of B atoms can be found (pentaborates, tetraborates, triborates, etc.). Bearing in mind the previous assertion as well as FTIR results, the presence of other borate species cannot be discarded.

In order to further characterise the natural mineral used as a binder for ceramic paper, XRD analyses were carried out. Fig. 3b shows XRD diffraction patterns of natural ulexite. In addition, the XRD patterns of pure ulexite, both before and after the elutriation treatment, are shown. Before the elutriation and drying processes, pure ulexite shows all XRD peaks that correspond to $NaCaB_5O_6(OH)_6\cdot 5H_2O$. Also, the presence of NaCl is evidenced according to XRF results. After the elutriation process, structural changes occur, which involve the loss of water and the appearance of less crystalline phases [13].

Thermal decomposition of ulexite occurs in different steps that involve dehydration, polymorphic transition and solid phase transformation. Fig. 4 shows TGA and SDTA profiles. The first step in the TGA profiles (Fig. 4a) occurs at temperatures <165 °C (Table 1, Δw_1) and it implies the loss of two water molecules ($NaCaB_5O_6(OH)_6\cdot 5H_2O \rightarrow NaCaB_5O_6(OH)_6\cdot 3H_2O + 2H_2O$). The second step (Table 1, Δw_2), observed between 165 °C and 185 °C, is associated with the loss of the three other water molecules ($NaCaB_5O_6(OH)_6\cdot 3H_2O \rightarrow NaCaB_5O_6(OH)_6 + 3H_2O$). Both steps correspond to dehydration processes. As Table 1 shows, both Δw_1 and Δw_2 are smaller than the theoretical values due to thermal treatment during binder conditioning. The third step involves the polymorphic transition $NaCaB_5O_6(OH)_6 \rightarrow NaCaB_5O_9 + 3H_2O$ that occurs at temperatures between 185 °C and 550 °C. Both natural ulexite and pure ulexite show Δw_3 values close to theoretical ones. A fourth step implies the crystallization process of $NaCaB_5O_9$, which is exothermic and it occurs at temperatures higher than 650 °C, but which does not imply changes in mass. At temperature close to 800–850 °C an endothermic peak indicates $NaCaB_5O_9$ decomposition ($NaCaB_5O_9 \rightarrow CaB_2O_4 + NaB_3O_5$). As reported by Garcia-Valles et al. [13], the position of this peak is affected by NaCl content. In the case of untreated pure ulexite, the thermal evolutions observed are the same as those previously described, though water loss steps at low temperatures are better defined (Fig. 4b).

The morphology of natural ulexite used as a binder for ceramic fibre was analyzed by SEM. Fig. 5 shows images of ceramic paper before and after calcination at 650 °C. A general view (Fig. 5a) shows an open structure consisting of ceramic fibre, linked by ulexite particles. Ribbon shape fibres of cellulose, approximately 50–100 μm wide, help to form the fibrous structure. A closer view (Fig. 5b) shows groups of ulexite sticks ca. 10 μm long and 1 μm wide, mainly cumulated between fibre crossings. After calcination, ulexite particles begin to sinter (Fig. 5c and d), acting as binders for ceramic fibres and being the cause of the strength of ceramic paper,

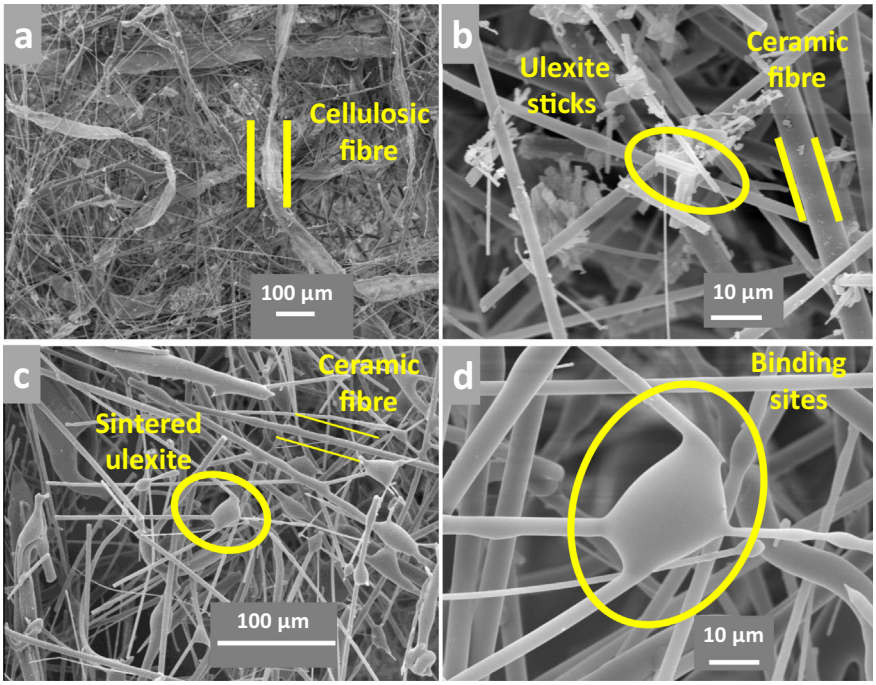

Fig. 5. SEM micrographs of ceramic paper, before (a and b) and after (c and d) first calcination.

as will be later discussed. As seen by TGA (Fig. 4), amorphous $NaCaB_5O_9$ is the species that appears to be joining ceramic fibres.

3.2. Catalytic species

After adding the catalytic phases, numerous aggregates deposit over ceramic fibres, preferably between fibre crossings (Fig. 6). In the case of PCer-La, wide clusters >10 μm size, are observed. The magnified view shows that lanthanum-species deposit over all ceramic fibres, and also smaller aggregates deposit on fibres. The presence of cracks indicates a shrinkage process during the drying-calcination step caused by crystallization processes. After cobalt and lanthanum addition (PCer-La,Co), oxidic clusters composed of smaller particles than those observed for PCer-La spread on ceramic fibres, and again mainly between fibre crossings. In addition, flakes ca. 1 μm long and particles ca. 100 nm distributed all along ceramic fibres are observed while they are not observed for PCer-La, which could indicate that they are probably formed by cobalt species.

In the case of PCer-Ba, the presence of filamentary structures, ca. 1 μm long and 50 nm in diameter is noticed, which appear to heterogeneously cover both ceramic fibres and sintered ulexite particles (Fig. 6). These filaments are perpendicular to the fibres (see magnified picture). When also adding cobalt, ceramic fibres appear to be completely covered by nanoparticles (50–100 nm) over which flakes deposit. No filaments associated with barium

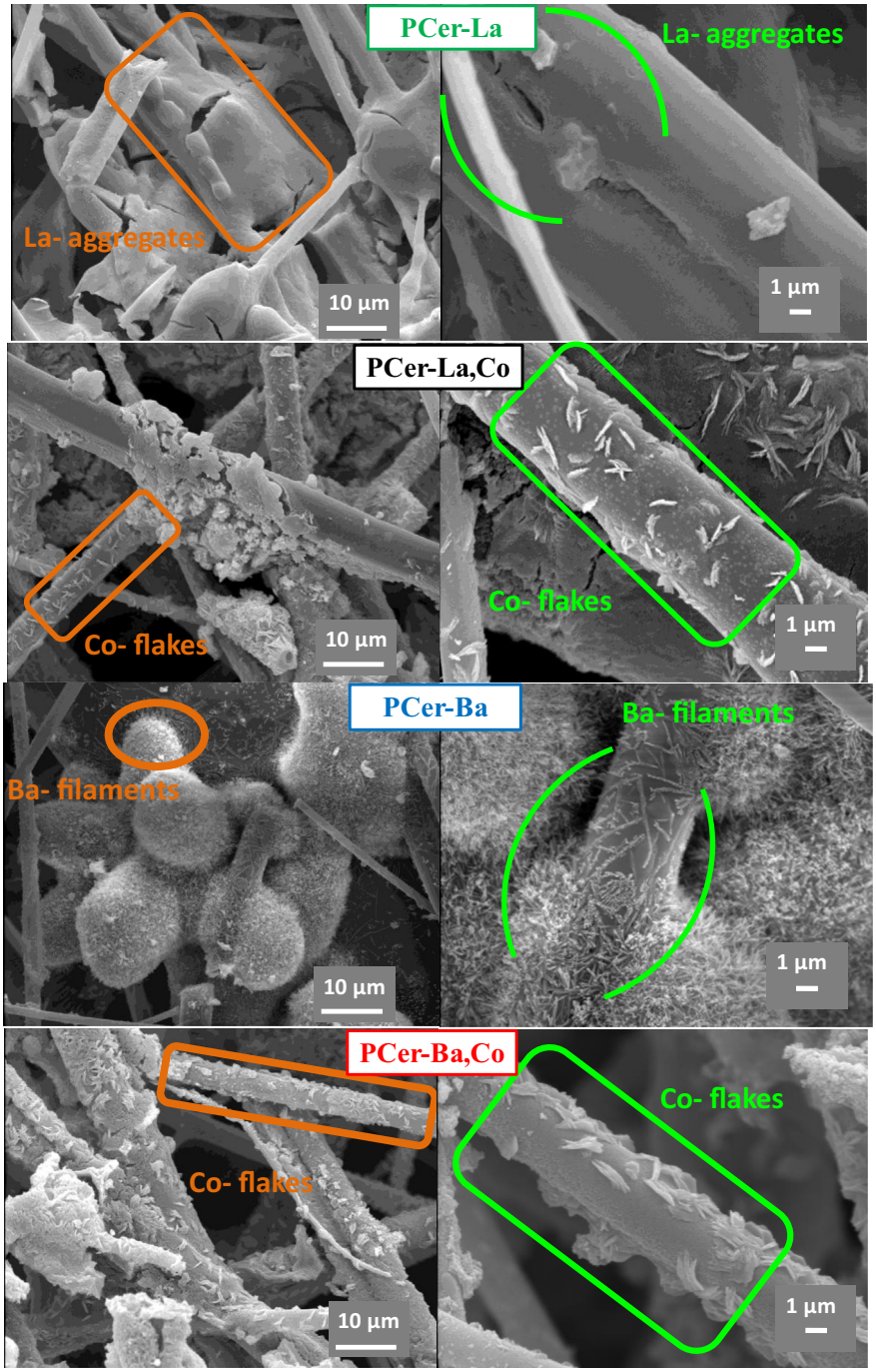

Fig. 6. SEM micrographs of catalytic systems at two magnifications.

species are observed for PCer-Ba,Co, but numerous oxidic aggregates turn up. The similarity of the flakes observed both for PCer-Ba,Co and PCer-La,Co suggests that flakes correspond to cobalt-containing species <100 nm.

In order to further characterise the species seen by SEM, several other techniques like FTIR, XRD, TGA and SDTA were used. Fig. 7 shows the IR spectra of catalytic ceramic paper both before and after catalytic tests. Fig. 7a displays the spectra of fresh samples (before catalytic tests). The spectrum of PCer is very similar to that of the bare ceramic fibres (two bottom profiles of Fig. 7a), despite the fact that signals associated with ulexite could be masked by the intense broad bands of ceramic fibres. PCer-La showed a signal at 1385 cm^{-1}, corresponding to NO_3^- species. After the addition of cobalt (PCer-La,Co), bands at 667 and 565 cm^{-1} associated with the Co-O bond stretching are observed, the former corresponding to Co^{2+} in tetrahedral coordination and the latter to Co^{3+} in octahedral coordination [26], which suggests the presence of Co_3O_4 (JCPDS-ICDD 9-418). Although the band at 1385 cm^{-1} is not observed for PCer-La,Co, it must be expected since Co_3O_4 catalyses nitrate decomposition [27]. The presence of La-carbonate species is not discarded either for PCer-La or PCer-La,Co, and very small signals may appear to be masked by the absorption bands of PCer. In the case of PCer-Ba, signals at 1437 and 858 cm^{-1} are observed due to the presence of $BaCO_3$ [27] whereas for PCer-Ba,Co, signals corresponding to Co_3O_4 emerge in addition to those of $BaCO_3$.

Fig. 7b illustrates IR spectra of used samples. In the case of PCer-La, signals at 1362, 1453 and 1510 cm^{-1}, corresponding to La $(NO_3)_3$ are observed [28] and for PCer-La,Co, besides those signals, others corresponding to Co_3O_4 are noted. On the other hand, PCer-Ba presents a spectrum similar to that of the fresh sample (Fig. 7a) though after catalytic test, signals associated with $BaCO_3$ are less intense. PCer-Ba,Co exhibits signals corresponding both to $BaCO_3$ and Co_3O_4.

Fig. 8 indicates XRD patterns of structured catalysts before (Fig. 8a) and after (Fig. 8b) catalytic tests. PCer fresh sample exposes an amorphous halo corresponding to ceramic fibres and natural ulexite calcined at 650 °C [19], while for Ba-containing samples, $BaCO_3$ (JCPDS-ICDD 45-1471) is detected and for La-containing paper, $La_2O_2CO_3$ (JCPDS-ICDD 23-322) is present. On the other hand, XRD patterns of Co-containing ceramic paper (PCer-Ba,Co and PCer-La,Co) exhibit Co_3O_4 signals. In the case of La-containing ceramic paper (PCer-La,Co and PCer-La), $La_2O_2CO_3$ signals are less intense for PCer-La,Co. As Fig. 8b proves, no significant differences are observed in the XRD patterns after catalytic test.

Fig. 9a shows TGA curves and Fig. 9b displays the corresponding SDTA profiles of non-calcined catalytic ceramic paper, i.e., ceramic paper loaded with a catalytic precursor without the final calcination treatment at 600 °C. TGA profiles can be divided into 4 zones: the first one for T < 200 °C, corresponding to dehydration processes. The second zone, between 200 °C and 270 °C, where a weight loss is observed for Co-containing samples (PCer-Ba,Co and PCer-La,Co), where correspondingly, in the SDTA profile, an endothermic evolution is noticed. This step corresponds to cobalt nitrate decomposition, according to: $3Co(NO_3)_2 \rightarrow Co_3O_4 + 6NO_2 + 1/2O_2$ [29]. Between 270 °C and 500 °C, a third zone can be distinguished, in which the evolution $La(NO_3)_3 + CO_2 \rightarrow La_2O_2CO_3 + 6NO_2 + 3/2O_2$ for La-containing ceramic paper (PCer-La and PCer-La,Co) is observed, which involves CO_2 coming from the air.

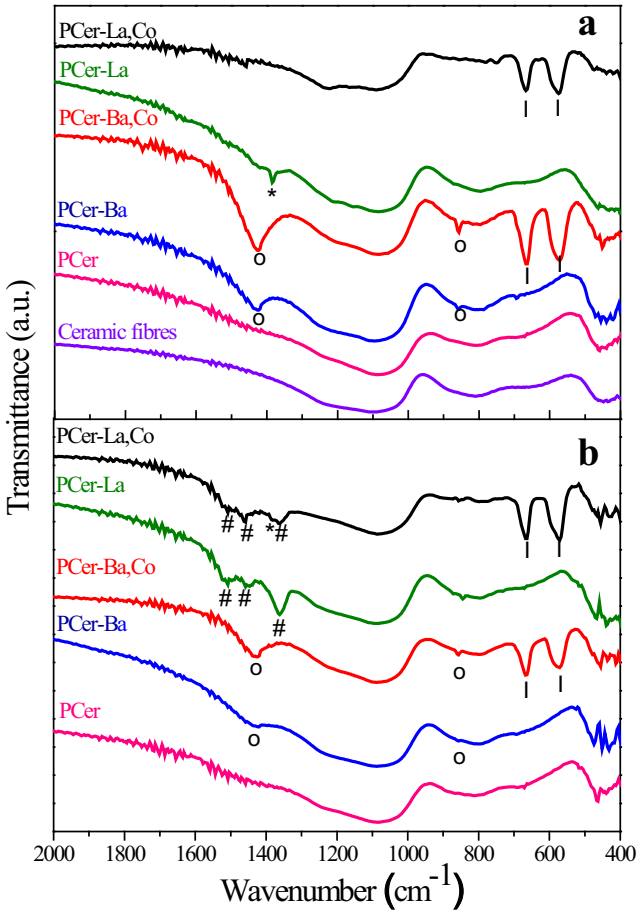

Fig. 7. Infrared spectra of catalytic systems: (a) before and (b) after TPO experiments. Symbols: * NO_3^-; # $La(NO_3)_3$; I Co_3O_4; o $BaCO_3$.

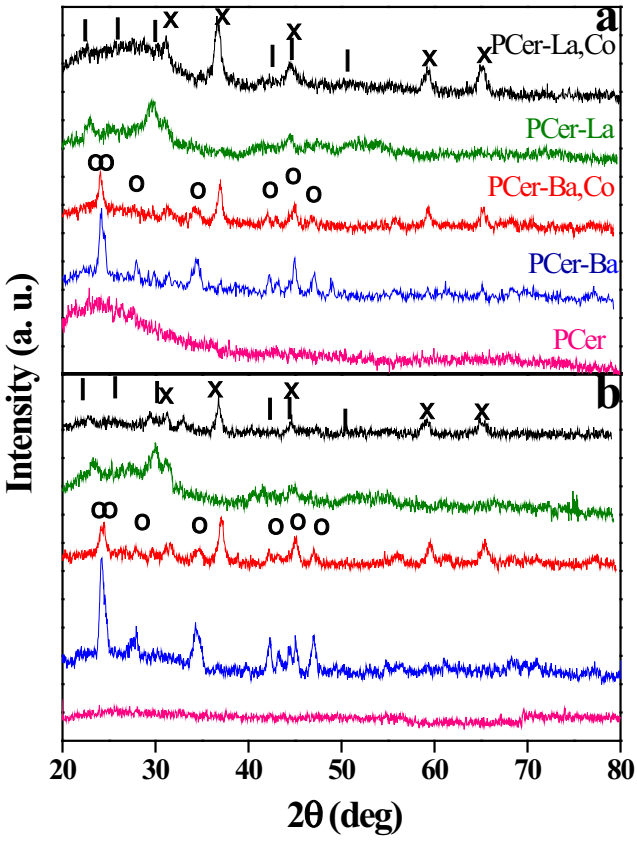

Fig. 8. XRD diffraction patterns of catalytic ceramic paper, (a) before catalytic run and (b) after evaluation. Symbols: I $La_2O_2CO_3$; * Co_3O_4; o $BaCO_3$.

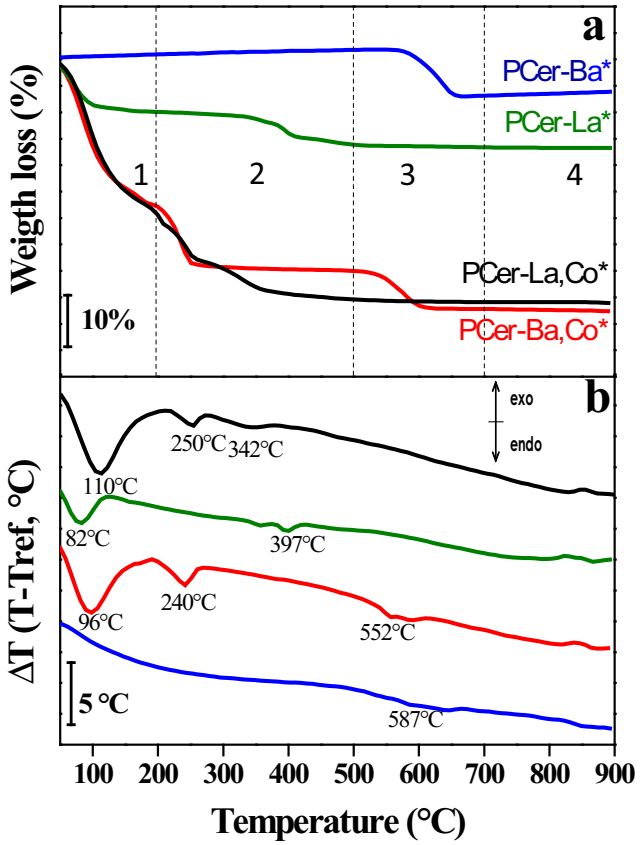

Fig. 9. Thermal analysis experiments of catalytic ceramic paper, (a) TGA and (b) SDTA. (Atmosphere: air and heating rate: 10 °C/min). The asterisk (*) indicates that catalytic ceramic paper has not been calcined at 600 °C after catalytic component addition.

Finally, in the fourth zone between 500 °C and 700 °C, the transformation $Ba(NO_3)_2 + CO_2 \rightarrow BaCO_3 + 2NO_2 + 1/2O_2$ can be noted. All these transformations involve endothermic processes (Fig. 9b) and the proposed transformations agree with characterisation results, as described above.

3.3. Strength and flexibility of ceramic paper

Mechanical properties are important for structured catalysts and especially for ceramic paper. Fig. 10 shows curves obtained with the INSTRON tester by plotting Tensile Load against Elongation. Tensile Indexes (TI, $N.m.g^{-1}$) and the Elastic Modules (MPa) were calculated from the maxima of the curves, i.e. breaking loads, and the slopes at the straight parts of the curves, respectively, as described in detail elsewhere [4]. A high tensile index and a low elastic modulus (high elasticity) are desirable to obtain strong, flexible and easy-to-handle ceramic paper. Since the two first parameters are conflicting ones, i.e. the stronger the ceramic paper, the less flexible it is, we focused on preparing ceramic paper strong and flexible enough for practical applications.

Fig. 10 indicates the complete curves since during these tests, paper tearing occurs and for this reason, each testing was carried out nine times at least, appearing in Fig. 10 the most representative curves. However, values reported in Table 2 are the average of values obtained during all the experiments performed, which are statistically consistent. The addition of the catalyst, either La,Co or Ba, Co, make catalytic ceramic paper less elastic but on the contrary, higher breaking loads are observed. This is evidenced in a higher Tensile Index value if PCer and PCer-La,Co are compared (0.90 N.

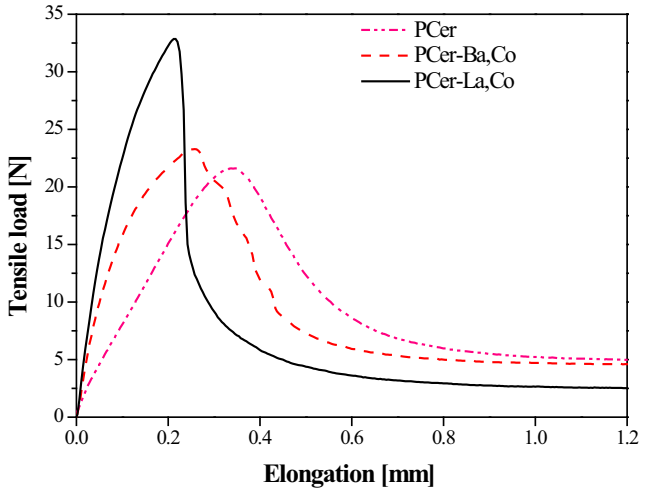

Fig. 10. Mechanical behaviour of ceramic and catalytic ceramic paper. Tensile values (TI) were obtained from the breaking load and the elastic module (EM) was calculated from the slope of the elastic portion of the curve.

Table 2
Mechanical properties of catalytic ceramic paper.

Ceramic paper	Tensile index* ($N.m.g^{-1}$)	Elastic module* (MPa)
PCer	0.90 ± 0.25	51.2 ± 10.21
PCer-Ba,Co	0.74 ± 0.09	67.7 ± 9.54
PCer-La,Co	1.02 ± 0.18	86.9 ± 6.88

* Values are indicated as mean values ± standard deviation.

$m.g^{-1}$ and 1.02 $N.m.g^{-1}$, respectively, Table 2). Nevertheless, in the case of PCer-Ba,Co, the Tensile Index value is lower, whereas the Breaking Load (Fig. 10) is higher. In this case, the increase in the grammage makes Tensile Index smaller (0.74 $N.m.g^{-1}$). As expected, after the addition of the catalyst the Elastic Modulus increases (i.e. elasticity decreases) from 51.2 MPa for PCer to 67.7 MPa for PCer-Ba,Co and 86.9 MPa for PCer-La,Co. If these values are compared with those corresponding to the ceramic paper prepared using conventional colloidal suspensions as a binder, reported by us in a previous contribution [4], natural ulexite makes ceramic paper stronger (higher tensile indexes) but less elastic (higher elastic modules). In spite of this, elasticity is less affected after catalyst addition for catalytic ceramic paper which has been prepared using natural ulexite instead of colloidal suspensions as binder. This aspect together with the lower cost of ulexite makes this borate compound an interesting substitute for colloidal suspensions.

Also, ceramic paper was prepared using pure ulexite to check its performance (Fig. 10). Both tensile index (0.12 $N.m.g^{-1}$) and elastic modulus (7.7 MPa) were similar to those of the ceramic paper prepared using a commercial CeO_2 colloidal suspension (Nyacol) (0.15 $N.m.g^{-1}$ and 3.2 MPa, respectively) [4]. However, as stated above, the yield in production of pure ulexite from the natural mineral is very low and in addition, natural ulexite allowed us to prepare stronger ceramic paper, for which the latter was chosen as a binder of ceramic fibres.

3.4. Catalytic activity

The catalytic activity of ceramic paper was evaluated by TPO and results are shown in Fig. 11 and Table 3. When feeding only diluted O_2 (Fig. 11a), all catalytic ceramic paper exhibited broad

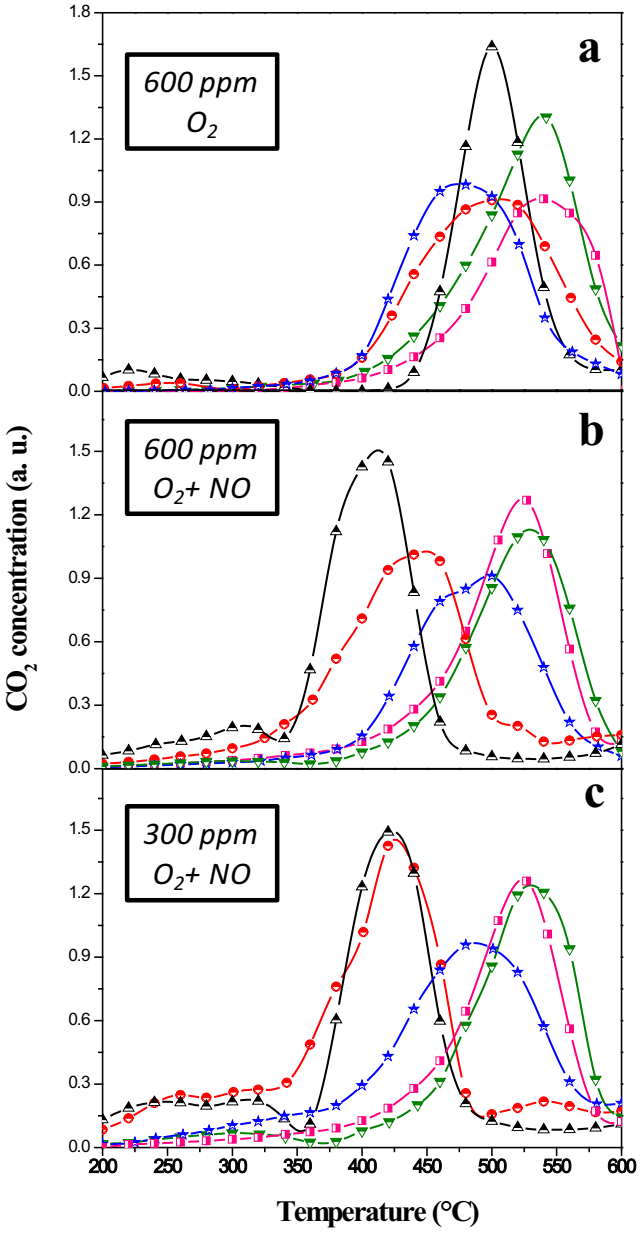

Fig. 11. Catalytic activity. TPO profile of diesel soot combustion. Effect of soot loading and NO presence. Conditions: (a) O_2 flow, soot suspension 600 ppm; (b) O_2 + NO flow, soot suspension 600 ppm, (c) O_2 + NO flow, soot suspension 300 ppm. —■— PCer, —★— PCer-Ba, —●— PCer-Ba,Co, —▼— PCer,La and —▲— PCer-La,Co.

Table 3
Diesel soot combustion activity (TPO).

Ceramic paper	600 ppm; O_2 T (°C)	600 ppm; O_2 + NO T (°C)	300 ppm; O_2 + NO T (°C)
PCer	540	527	525
PCer-La	542	520	530
PCer-La,Co	500	420	420
PCer-Ba	480	500	480
PCer-Ba,Co	500	440	420

TPO peaks, with maxima between 475 and 550 °C. Both PCer and PCer-La are practically non-active, whereas Co-containing ceramic paper show TPO profiles shifted toward lower temperatures. Unexpectedly, the TPO curve corresponding to PCer-Ba was the most active catalyst which showed the maximum of the curve at 480 °C. This fact could be related to the presence of adsorbed NO_2 species for Ba-containing samples. Characterisation results indicated that $BaCO_3$ was the species formed after the calcination treatment of PCer-Ba. Considering that the precursor salt used for the preparation of the latter was $Ba(NO_3)_2$ and according to a previous work [27], part of NOx released during the calcination step could remain adsorbed on the catalyst surface as O-Ba—NO_2 and released when heating under the TPO run. The fibrous nature of the catalytic ceramic paper matrix makes it difficult to detect this species by FTIR. In order to further confirm this, Fig. 2S (Supplementary Information) shows stability TPO runs obtained for PCer-Ba when NO is not present in the feeding. Although the first run apparently indicates a high activity of this sample, the following ones are shifted to the right. On the other hand, in the case of PCer-Ba,Co, the TPO peak could be convoluted from two contributions, the former with a maximum at 480 °C, which coincides with that observed for PCer-Ba, and the latter with a maximum at 500 °C. This could be explained through the partial decomposition of nitrates due to the presence of Co_3O_4 [27].

In the presence of NO (usually present in diesel exhaust gases), i.e., when feeding NO + O_2 (Fig. 11b), better activities are observed. All curves shifted to lower temperatures, especially those corresponding to Co-containing catalytic ceramic paper. Maxima observed in the TPO profile are 420 °C and 440 °C for PCer-La,Co and PCer-Ba,Co, respectively. This could be associated with the presence of Co_3O_4 (as previously seen by FTIR, XRD and TGA), homogeneously distributed all along ceramic fibres. This could favour the formation of NO_2, a more powerful oxidant than O_2, and establish a redox cycle between NO_2 and NO. Ba-containing ceramic paper exhibited wider peaks, probably due to barium carbonate nitration during the TPO run, according to the reaction: $BaCO_3 + NO_2 + O_2 \rightarrow Ba(NO_3)_2 + CO_2$. CO_2 thus released adds to that formed by the soot combustion producing a broad TPO peak. The addition of lanthanum did not cause any significant enhancement of the activity (the maximum in the TPO profile is the same for PCer and PCer-La, Table 3, 1st and 2nd columns).

Apart from what has been discussed above, great amounts of soot could hinder the contact between the soot and the catalyst. For this reason, catalytic ceramic paper discs were also evaluated after impregnation of soot from a less concentrated suspension (300 ppm of soot in n-hexane). In this way, TPO curves result narrower (Fig. 11c) and the maximum soot combustion for Co-containing samples appears at 420 °C, being this temperature close to that of diesel exhaust gases. Besides these differences, the temperatures for the maximum combustion rate were similar; indicating that the contact reached in both cases was similar. The activity accomplished with these Co-containing catalytic ceramic paper is similar to that of Co,Ce and better than that of Co,Ba,K coated on ceramic monoliths, despite the absence of potassium that enhances the catalyst-to-soot contact, but which is lost at high temperature and in the presence of water [30]. This makes Ba,Co and La,Co ceramic paper, here reported, good candidates for the passive regeneration of a catalytic Diesel soot filter.

4. Conclusions

A simple and low-energy demanding method was developed to separate ulexite $NaCaB_5O_6(OH)_6{\cdot}5(H_2O)$ from the natural material extracted from the ulexite deposit (Salta, Argentina), in order to obtain an efficient binder material to join the fibres during the papermaking process used to obtain catalytic ceramic paper.

Natural ulexite, thus extracted, allowed for the production of ceramic paper with mechanical properties suitable for handling and adapting them to containers of different geometries. The

replacement of colloidal suspensions by this mineral constitutes a step forward in the development of ceramic paper.

When the catalytic components were added, La produced aggregates mainly of $La_2O_2CO_3$, barium was deposited in the form of $BaCO_3$ filaments, and the further addition of cobalt produced flakes of Co_3O_4.

The catalytic ceramic paper developed proved to be active for diesel soot combustion at a low temperature and it can be considered a potential candidate for the passive regeneration of diesel particulate filters. The best activities were obtained with Co-containing ceramic paper, i.e. Co,Ba or Co,La, being the role of the basic compound to trap NO_x and to yield reactive oxygen to the Co-soot centres, while the role of the transition element was to promote soot oxidation through its redox capacity.

Acknowledgements

The authors wish to acknowledge the financial support received from ANPCyT, CONICET, SECTEI Santa Fe and UNL. Thanks are also offered to BORAX S.A. for supplying the borate mineral.

Appendix A. Supplementary data

Supplementary data associated with this article can be found, in the online version, at http://dx.doi.org/10.1016/j.cej.2017.02.013.

References

[1] E. Reichelt, M.P. Heddrich, M. Jahn, A. Michaelis, Fibre based structured materials for catalytic applications – review, Appl. Catal. A 476 (2014) 78–90.
[2] Q. Liu, T. Xue, L. Yang, X. Hu, H. Du, Controllable synthesis of hierarchical porous mullite fibre network for gas filtration, J. Eur. Ceram. Soc. 36 (2016) 1691–1697.
[3] H. Koga, H. Ishihara, T. Kitaoka, A. Tomoda, R. Suzuki, H. Wariishi, NO_X reduction over paper-structured fibre composites impregnated with Pt/Al_2O_3 catalyst for exhaust gas purification, J. Mater. Sci. 45 (2010) 4151–4157.
[4] F.E. Tuler, E.D. Banús, M.A. Zanuttini, E.E. Miró, V.G. Milt, Ceramic papers as flexible structures for the development of novel diesel soot combustion catalysts, Chem. Eng. J. 246 (2014) 287–298.
[5] J.P. Cecchini, E.D. Banús, S.A. Leonardi, M.A. Zanuttini, M.A. Ulla, V.G. Milt, Flexible structured systems made of ceramic fibres containing Pt-NaY zeolite used as CO oxidation catalysts, J. Mater. Sci. 50 (2) (2014) 755–768.
[6] Y. Shiratori, T. Quang-Tuyen, K. Sasaki, Performance enhancement of biodiesel fueled SOFC using paper-structured catalyst, Int. J. Hydrogen Energy 38 (2013) 9856–9866.
[7] Y. Shiratori, T. Ogura, H. Nakajima, M. Sakamoto, Y. Takahashi, Y. Wakita, T. Kitaoka, K. Sasaki, Study on paper-structured catalyst for direct internal reforming SOFC fueled by the mixture of CH_4 and CO_2, Int. J. Hydrogen Energy 38 (2013) 10542–10551.
[8] Y. Shiratori, T. Quang-Tuyen, Y. Umemura, T. Kitaoka, K. Sasaki, Paper-structured catalyst for the steam reforming of biodiesel fuel, Int. J. Hydrogen Energy 38 (2013) 11278–11287.
[9] J.P. Bortolozzi, E.D. Banús, D. Terzaghi, L.B. Gutierrez, V.G. Milt, M.A. Ulla, Novel catalytic ceramic papers applied to oxidative dehydrogenation of ethane, Catal. Today 216 (2013) 24–29.
[10] H. Koga, T. Kitaoka, M. Nakamura, H. Wariishi, Influence of a fibre-network microstructure of paper-structured catalyst on methanol reforming behaviour, J. Mater. Sci. 44 (2009) 5836–5841.
[11] H. Ichiura, N. Okamura, T. Kitaoka, H. Tanaka, Preparation of zeolite sheet using a papermaking technique Part II: the strength of zeolite sheet and its hygroscopic characteristics, J. Mater. Sci. 36 (2001) 4921–4926.
[12] J.P. Cecchini, R.M. Serra, M.A. Ulla, M.A. Zanuttini, V.G. Milt, Enhancing mechanical properties of ceramic papers loaded with zeolites using borate compounds as binders, BioResearch 8 (1) (2013) 313–326.
[13] M. Garcia-Valles, P. Alfonso, J.R.H. Arancibia, S. Martínez, D. Parcerisa, Mineralogical and thermal characterization of borate minerals from Rio Grande deposit, Uyuni (Bolivia), J. Therm. Anal. Calorim. 125 (2) (2016) 673–679.
[14] S. Stefanov, Applications of borate compounds for the preparation of ceramic glazes, Glass Technol. 41 (2000) 193–196.
[15] A. Christogerou, T. Kavas, Y. Pontikes, S. Koyas, Y. Tabak, Angelopoulos GN "Use of boron wastes in the production of heavy clay ceramics", Ceram. Int. 35 (2009) 447–452.
[16] V.S. Nandi, F. Raupp-Pereira, O.R.K. Montedo, A.P.N. Oliveira, The use of ceramic sludge and recycled glass to obtain engobes for manufacturing ceramic tiles, J. Clean. Prod. 86 (2015) 461–470.
[17] Z.B. Ozturk, Thermal behavior of transparent wall tile glazes containing ulexite, J. Aust. Ceram. Soc. 51 (2) (2015) 69–74.
[18] G. Guzel, O. Sivrikaya, H. Deveci, The use of colemanite and ulexite as novel fillers in epoxy composites: influences on thermal and physico-mechanical properties, Compos. B 100 (2016) 1–9.
[19] S. Şener, G. Özbayoğlu, Ş. Demirci, Changes in the structure of ulexite on heating, Thermochim. Acta 362 (2000) 107–112.
[20] H.R. Flores, S.K. Valdez, Thermal requirements to obtain calcined and frits of ulexite, Thermochim. Acta 452 (2007) 49–52.
[21] <http://minerals.stage.riotintodev.com/documents/RTM.SiteMap.Sept2011.pdf>.
[22] S. Kutuk, Influence of milling parameters on particle size of ulexite material, Powder Technol. 301 (2016) 421–428.
[23] M. Piumetti, S. Bensaid, N. Russo, D. Fino, Investigations into nanostructured ceria–zirconia catalysts for soot combustion, Appl. Catal. B 180 (2016) 271–282.
[24] H. Ichiura, Y. Kubota, Z. Wu, H. Tanaka, Preparation of zeolite sheets using a papermaking technique Part I dual polymer system for high retention of stock components, J. Mater. Sci. 36 (2001) 913–917.
[25] L. Jun, X. Shuping, G. Shiyang, FT-IR and Raman spectroscopic study of hydrated borates, Spectrochim. Acta 51A (4) (1995) 519–532.
[26] A.D. Khalaji, M. Nikookar, K. Fejfarova, M. Dusek, Synthesis of new cobalt (III) Schiff base complex: a new precursor for preparation Co_3O_4 nanoparticles via solid-state thermal decomposition, J. Mol. Struct. 1071 (2014) 6–10.
[27] V.G. Milt, C.A. Querini, E.E. Miró, M.A. Ulla, Abatement of diesel exhaust pollutants: NOx adsorption on Co, Ba, K/CeO_2 catalysts, J. Catal. 220 (2003) 424–432.
[28] E.D. Ion, B. Malič, I. Arčon, J. Padežnik Gomilšek, A. Kodre, M. Kosec, Characterization of lanthanum zirconate prepared by a nitrate-modified alkoxide synthesis route: from sol to crystalline powder, J. Eur. Ceram. Soc. 30 (2010) 569–575.
[29] V.G. Milt, M.A. Ulla, E.E. Miró, NO_x trapping and soot combustion on $BaCoO_{3-y}$ perovskite: LRS and FTIR characterization, Appl. Catal. B 57 (2005) 13–21.
[30] F.E. Tuler, R. Portela, P. Ávila, J.P. Bortolozzi, E.E. Miró, V.G. Milt, Development of sepiolite/SiC porous catalytic filters for diesel soot abatement, Microporous Mesoporous Mater. 230 (2016) 11–19.